

Content from this work may be used under the terms of the CC BY 3.0 licence (© 2019). Any distribution of this work must maintain attribution to the author(s), title of the work, publisher, and DOI.

# COMPARISON OF THE LATTICE THERMAL CONDUCTIVITY OF SUPERCONDUCTING TANTALUM AND NIOBIUM

Peng Xu, Neil T. Wright, Mechanical Engineering  
 Thomas R. Bieler, Chemical Engineering and Materials Science  
 Michigan State University, East Lansing, MI48823, USA

## Abstract

The thermal conductivity  $k$  of superconducting tantalum (Ta) behaves similarly to that of superconducting niobium (Nb), albeit at colder temperatures. This shift is due to the superconducting transition temperature of Ta being 4.48 K, versus 9.25 K for Nb. For example, the temperature of the phonon peak of properly treated Ta is about 1 K as opposed to a phonon peak at about 2 K for Nb. The typical value of  $k$  of Ta is smaller than Nb with the value at the phonon peak for Ta being  $O(10) \text{ W m}^{-1} \text{ K}^{-1}$ . Like Nb,  $k$  is dominated by phonons at these temperatures. This lattice  $k$  can be modeled by the Boltzmann transport equation, solved here by a Monte Carlo method using the relaxation time approximation. The phonon dispersion relation is included and some of the individual scattering mechanisms due to boundaries, dislocations, and residual normal electrons are examined. Differences in the thermal response of deformed Ta, as compared with Nb, may be attributed to differences in dislocation densities of the two metals following similar levels of deformation. Boundary scattering dominates at the coldest temperatures. The phonon peak decreases and shifts to warmer temperatures with increasing deformation.

## INTRODUCTION

Manufacturing superconducting radio frequency (SRF) cavities from large grain Nb sheets may reduce cost and improve their quality factor [1]. However, manufacturing SRF cavities from Nb sheets requires large deformations that increase dislocation density [2], which has been shown to reduce the thermal conductivity of superconducting large grain Nb [3–5]. Good thermal conductivity  $k$  is critical for mitigating heat generation during superconducting conditions. Thus, developing models for designing cavity fabrication paths that can maximize  $k$  is important to prevent cavity quench, thus improving cavity performance [6].

Ta is a part of the refractory metals group and also a superconducting metal, similar to Nb. Because Nb and Ta are found together, there is always Ta present in SRF cavities, this provides some intrinsic interest and motivation for understanding the thermal conductivity of Ta. Ta and Nb behave like twins in nature and they have very similar physical and chemical properties. For example, both of them are body-center cubic materials and have similar thermal conductivity at room temperature. However, the transition temperature ( $T_c$ ) from normal conductor to superconductor of Ta is 4.48 K, which is about one half of that of Nb ( $T_c = 9.25 \text{ K}$ ) [7].

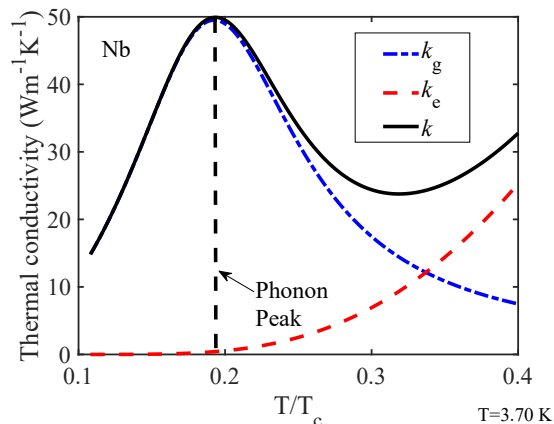


Figure 1: Phonon and electron contributions to the thermal conductivity of undeformed superconducting Nb.

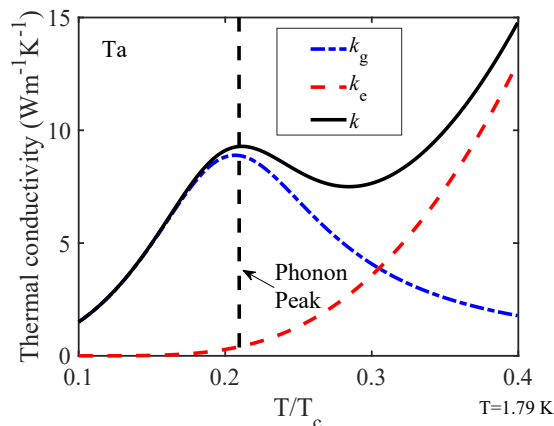


Figure 2: Phonon and electron contributions to the thermal conductivity of undeformed superconducting Ta.

The thermal conductivity of superconducting metals is described as the sum of an electronic component  $k_e$  and a lattice vibration component  $k_g$  [8]. Typical examples of thermal conductivity contributions for undeformed Nb and Ta are shown in Figs. 1 and 2, respectively. For  $T/T_c < 0.2$ , phonon contributions to the thermal conductivity dominate over the electronic contributions. The purity of the metal (i.e., RRR) largely determines the electronic component  $k_e$ . A number of factors, including sample size, specularly, free electrons, impurity concentration, and dislocation density  $N_d$ , determine  $k_g$ . Plastic deformation, which occurs in many manufacturing processes, increases  $N_d$ , while heat treatments may reduce  $N_d$  [5].

## MODELS OF THERMAL CONDUCTIVITY

**Parameterization** The thermal conductivity of superconducting Nb and Ta can be modeled as the sum of electron transport of energy and phonon transport of energy. In normally conducting metals, the phonon part is usually negligible due to scattering by normal electrons. However, in the superconducting regime, the formation of electrons into Cooper pairs leads to a reduction in the electron contribution to energy transport as well as a reduction in scattering of phonons by electrons [9, 10]. Therefore, the phonon contribution dominates the thermal conductivity for temperatures below  $T/T_c = 0.2$ , where the electronic contributions are almost 0, as shown in Fig. 1 and Fig. 2.

Xu et al. [11] proposed a model based on the Koechlin and Bonin [12] parameterization (K& B model) of the thermal conductivity of superconducting materials by explicitly including a term for phonon-dislocation scattering, where the K& B model is based on the BRT [10] expression according to the BCS theory [9]. The expression of the model proposed by Xu et al. is

$$k = R(y) \left[ \frac{\rho}{LT} + aT^2 \right]^{-1} + \left[ \frac{1}{D \exp(y)T^2} + \frac{1}{B\Lambda T^3} + \frac{KN_d}{T^2} \right]^{-1} \quad (1)$$

where  $KN_d/T^2$  is the term added to account for the effect of phonon-dislocation scattering.  $R(y)$  quantifies the condensation of normal conducting electrons into Cooper pairs [10],  $\rho$  is the residual resistivity.  $L$  is the Lorentz number,  $a$  is the coefficient of momentum exchange of electrons with the lattice,  $D$  refers to phonon-electron scattering,  $B$  corresponds to phonon-boundary scattering,  $\Lambda$  is the phonon mean free path. The term  $y$  in  $R(y)$  is defined as

$$y = \frac{\Delta(T)}{k_B T} = \frac{\Delta(T)}{k_B T_c} \frac{T_c}{T} \quad (2)$$

where  $\Delta(T)$  is the superconducting energy gap, and  $k_B$  the Boltzmann constant. For  $T/T_c < 0.6$ ,  $y$  can be approximated as  $y = \alpha T_c/T$ ,  $\alpha \approx 1.76$  in BCS theory but may take different values according to experiments on different metals [12], and  $\rho$ ,  $a$ ,  $B$ ,  $\alpha$ ,  $D$ , and  $N_d$  are the parameters that need to be determined. The resistivity  $\rho$  and dislocation density may be determined by measurements. The two terms in  $k_e$  are due to electron-defect scattering and electron-phonon scattering, respectively, and the three terms in  $k_g$  are due to phonon-electron scattering, phonon boundary scattering, and phonon-dislocation scattering, respectively.

The parameter  $K$  is expressed following Klemens [13] for randomly distributed dislocations as

$$K = \frac{0.038(\bar{v}h^2)b^2\gamma^2}{k_B^3} \quad (3)$$

where  $\gamma$  is the Grüneisen constant,  $b$  is the Burgers vector,  $\bar{v}$  is the average group velocity,  $h$  is the Planck constant and  $k_B$  is the Boltzmann constant.

Comparison of data from [3] with fitting of Eq. (1) are shown in Fig. 3 for an undeformed sample and Fig. 4 for the

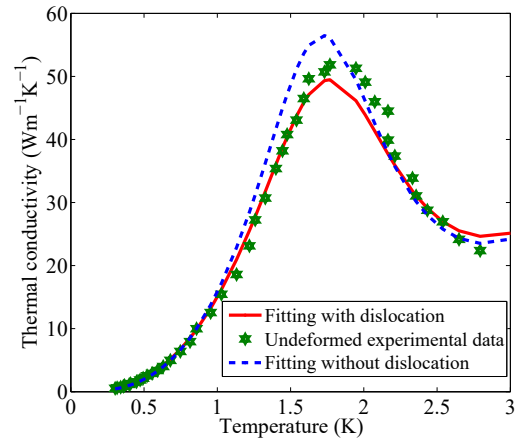


Figure 3: Comparison between fitting with or without dislocation term for undeformed Nb sample from [3]. Calculated dislocation density is  $N_d = 4.7 \times 10^{12} \text{ m}^{-2}$ .

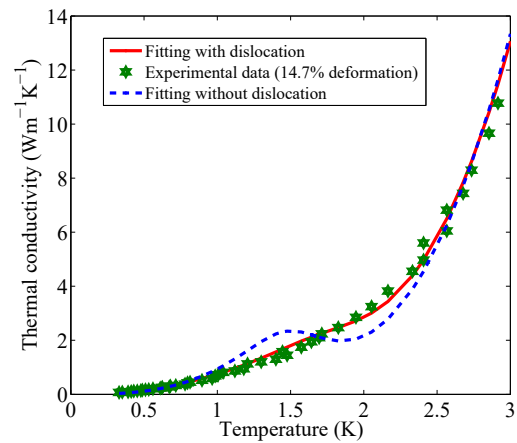


Figure 4: Comparison between fitting with or without dislocation term for deformed Nb sample [3]. Calculated dislocation density is  $N_d = 3.8 \times 10^{14} \text{ m}^{-2}$ .

same sample after a uniaxial Cauchy strain of 14.7%. When the dislocation term is included in the fit, the qualitative and quantitative agreement with the experimental results [3] improves significantly, especially for Nb after deformation. Koechlin and Bonin noticed a discrepancy during their fitting with the experimental results. This deviation may have been due to the lack of a phonon-dislocation scattering term in their model.

**Monte Carlo Simulation** The Boltzmann transport equation (BTE) has been widely used to model phonon and electron transport. The BTE for phonon transport can be written as [14]

$$\frac{\partial f}{\partial t} + v_g \cdot \Delta f = \left[ \frac{\partial f}{\partial t} \right]_{scat} \quad (4)$$

where  $f(r, q, t)$  is the distribution function of an ensemble of phonons, a function of position ( $r$ ), time ( $t$ ), and wave vector

Table 1: Parameters of the Samples Examined [3, 7].  $\epsilon$ -Cauchy Strain

Sample	RRR	$N_d \times 10^{12} \text{m}^{-2}$ ( $\epsilon$ )				
Nb1	350	4.49 (0%)	5.91 (8%)			
Nb2	1200	0.0611 (0%)	14 (4%)	159 (8%)		
Nb3	250	5.11 (0%)	8.64 (3%)	47.6 (7.3%)	157 (10.3%)	367 (14.7%)
Ta1	185	0.0297 (0%)	11.9 (2%)	19.9 (3.1%)	108 (7.3%)	
Ta2	111	0.105 (0%)	30.1 (1.2%)	66.6 (2.4%)	123 (3.9%)	211 (6.2%)
Ta3	60	0.0173 (0%)	0.489 (1%)	482 (10%)		

( $q$ ), and  $v_g$  is the phonon group velocity. The left-hand side of Eq. (4) represents the change of the distribution function due to motion or drift, and the right-hand side represents the change due to collision or scattering. Due to the complex nature of scattering events, a relaxation time approximation is often used to simplify the scattering term by writing

$$\left[ \frac{\partial f}{\partial t} \right]_{scat} = \frac{f - f_0}{\tau} \quad (5)$$

where  $\tau$  is the overall relaxation time,  $f_0$  is the phonon distribution function at equilibrium. The relaxation time is due to several scattering mechanisms, including phonon-phonon scattering, phonon-impurity scattering, phonon-boundary scattering, phonon-electron scattering, and phonon-dislocation scattering, etc. The distribution function  $f(r, q, t)$  is a function of seven independent variables, including time ( $t$ ), three space variables ( $r$ ), and three wave-vector variables ( $q$ ). In addition, the scattering mechanisms are usually nonlinear functions. These complexities render the solution of the BTE extremely difficult by deterministic means [14].

The Monte Carlo method is a stochastic method to solve the BTE and has been widely used for phonon and electron transport [14–17]. As the thermal conductivity of Nb and Ta at superconducting temperature is dominated by phonon contributions, the Monte Carlo simulation method is suitable to model the lattice thermal conductivity of superconducting Nb and Ta. An energy-based, variance-reduced Monte Carlo method [17] is used in this paper. This method only models the deviation in the energy of a particle population from its nearby equilibrium, with the equilibrium described analytically. This saves significant computational cost as compared with standard methods because calculations start relatively close to equilibrium.

In the Monte Carlo simulation, the phonon-boundary scattering is treated during the drift process, *i.e.*, when a phonon reaches the physical boundary of a sample, it reflects back either specularly or diffusively, depending on the specularly of the surface. Scattering with dislocations can be treated similarly to the isotropic scattering of photons when addressing thermal radiation. Scattering of phonons due to the anharmonic terms of the potential (*i.e.*, electrons) tends to restore thermal equilibrium.

Please refer to [18] for details of the Monte Carlo solution technique, including initialization, drift process, scattering process, and calculating the thermal conductivity.

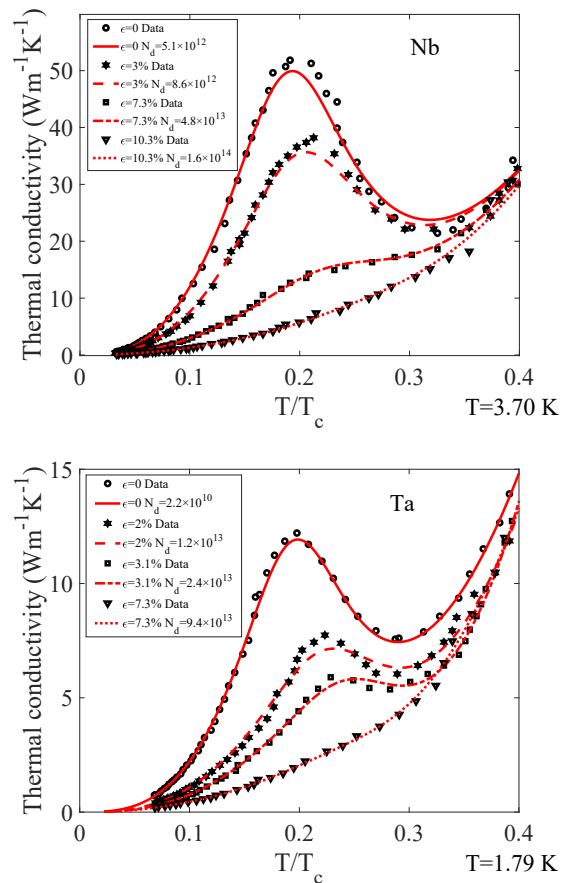


Figure 5: Comparison between the data of the thermal conductivity of deformed superconducting metals (symbols) and the best fit using Eq. (1) (lines). Top panel is Nb [3], for  $\epsilon = 0\%$ ,  $3\%$ ,  $7.3\%$ , and  $10.3\%$  and bottom panel is Ta [7], for  $\epsilon = 0\%$ ,  $2\%$ ,  $3.1\%$ , and  $7.3\%$ . The dislocation density is calculated during the fitting process

## RESULTS AND DISCUSSION

Equation 1 improves agreement with the experimental results as compared with the model w/o dislocation term [12].

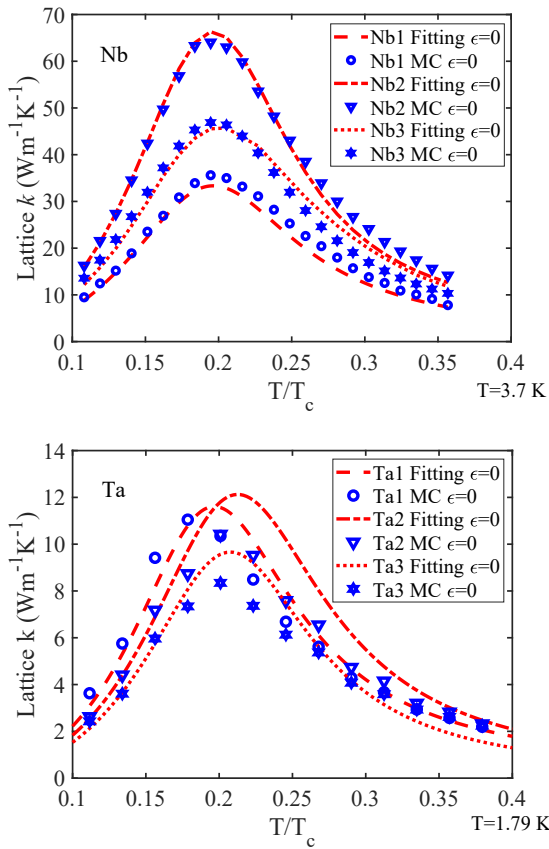


Figure 6: Monte Carlo solution of Eq. (4) (symbols) compared with the best fit of Eq. (1) (lines) for the lattice thermal conductivity of three undeformed Nb samples [3] (top panel) and three undeformed Ta samples [7] (bottom panel). The parameters (size, RRR, deformation temperature, and estimated  $N_d$ ) for each sample are listed in Table 1.

Comparison of data from [3, 19] with fitting of using Eq. (1) is shown in Fig. 5 for superconducting Nb and superconducting Ta, both before and after deformation. The figures show that after deformation, the thermal conductivity of both Nb and Ta decrease because of the increase of dislocation density, where the temperatures at the phonon peak ( $T_{pp}$ ) increase with deformation for both Nb and Ta. The phonon peak disappears after 7.3% deformation for these Nb and Ta samples. After 10.3% deformation for this Nb sample, the thermal conductivity increases proportionally with temperature. Another interesting similarity between Nb and Ta is that  $k_{pp}$  occurs at  $T/T_c \approx 0.2$  and  $k_{min}$  (local minimum) occurs at  $T/T_c \approx 0.3$  for both Nb and Ta. However, at  $T/T_c \approx 0.4$ , the thermal conductivity of Ta is greater than the value at the phonon peak, while the thermal conductivity of Nb is smaller than the value at its phonon peak.

Monte Carlo simulation results of the lattice thermal conductivity of superconducting Nb and Ta samples before deformation are shown in Fig. 6, and compared with the fit of Eq. (1). The simulation results match well with fitting results by including the effect of phonon-boundary scattering,

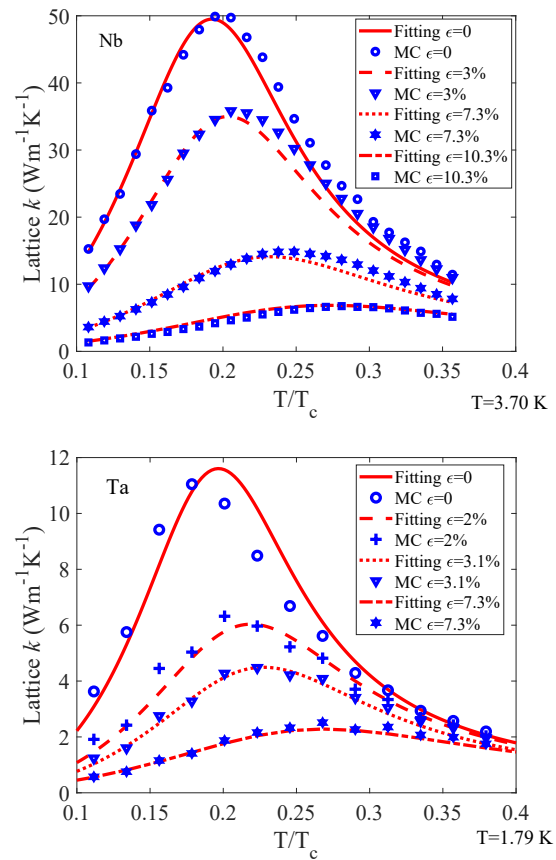


Figure 7: Monte Carlo solution of Eq. (4) (symbols) compared with the best fit of Eq. (1) (lines) for the lattice thermal conductivity of deformed sample Nb3 [3] (top panel) with  $\epsilon = 0\%$ , 3%, 7.3%, and 10.3% and deformed sample Ta1 [7] (bottom panel) with  $\epsilon = 0\%$ , 2%, 3.1%, and 7.3%. The parameters (size, RRR, deformation temperature, and estimated  $N_d$ ) for each sample are listed in Table 1.

tering, phonon-electron scattering and phonon-dislocation scattering. Here, the phonon-dislocation scattering is less important for undeformed samples with the other two scattering mechanisms. It can be also seen from the simulation results that the phonon peak appears at about 1.8 K for Nb and 0.9 K for Ta for all of the three samples. The temperature at the phonon peak is close to  $0.2 T_c$ . Therefore the phonon peak at the undeformed Nb and Ta has small variations.

Simulation results of the lattice thermal conductivity of superconducting Nb and Ta samples after deformation are shown in Fig. 7, and compared with the fit of Eq. (1). The simulation results also match well with fitting results by including the effect of phonon-boundary scattering, phonon-electron scattering and phonon-dislocation scattering. Here, the phonon-dislocation scattering is more important for deformed samples with the other two scattering mechanisms, due to the increase of dislocation density after deformation. Wasserbach observed that sample Nb1 has predominantly screw dislocations while Nb2 has predominantly edge dislocations. He also found that low T ( $T < 295$  K) deformation

leads to screw dislocations, and intermediate temperature ( $295\text{ K} < T < 475\text{ K}$ ) deformation results in edge dislocations [3]. As the Ta samples are deformed at  $T > 295\text{ K}$ , which falls into the intermediate temperature range, they are likely have edge dislocations [19]. It is shown from the figure that  $k_{pp}$  decreases with deformation and will eventually disappear after large deformation, while  $T_{pp}$  increases with deformation for both Nb and Ta. These results can be accounted for by the effect of dislocations. It can be also seen that the lattice thermal conductivity of Nb has greater value than Ta in similar conditions. It is not difficult to find that for a given deformation, the ratio of the thermal conductivity to the undeformed state ( $k/k_{\epsilon=0}$ ) for Ta is smaller than that in Nb.

## CONCLUSIONS

Thermal conductivity of superconducting Nb are critical to the performance of SRF cavities. At the working temperature of SRF cavities, phonon-dislocation scattering plays an important role to affect the thermal conductivity of superconducting metals for samples after deformation. Wasserbäch carefully examined each of the phonon scattering mechanisms to the thermal conductivity with particular attention to dislocations. Analysis of the thermal conductivity of superconducting metals shows that in addition to  $k_{pp}$  decreasing after deformation, there is a shift increase in  $T_{pp}$ . The proposed expression combines different scattering mechanisms into an equation by adding a phonon-dislocation scattering term that improves the accuracy of fits to experimental data, especially for deformed samples at low temperatures. The proposed model can also be used to infer the dislocation density from measurements of  $k$ .

Monte Carlo simulation modeled the lattice thermal conductivity of superconducting Nb and Ta by including the effect of phonon-boundary scattering, phonon-electron scattering, and phonon-dislocation scattering. Simulation results match well with the proposed model Eq. (1). The phonon peak thermal conductivity appears at  $T \approx 1.8\text{ K}$  and at  $T \approx 0.9\text{ K}$  for undeformed Nb and Ta. It moves to warmer temperature after deformation until the phonon peak disappears. By comparing the thermal conductivity of Nb and Ta, it is found that Ta has a smaller thermal conductivity than similarly prepared Nb. For example, thermal conductivity at the phonon peak varies from 30 to  $60\text{ Wm}^{-1}\text{K}^{-1}$  for undeformed Nb examined in this paper at superconducting temperatures, while it varies from 10 to  $12\text{ Wm}^{-1}\text{K}^{-1}$  for undeformed Ta in similar conditions. Thermal conductivity decreases more readily for Ta than in Nb, and the reason might be due to the different dislocation mechanisms inside metals. As all the three Ta samples are deformed at a temperature equal or higher than 295 K, they are more likely have edge dislocations [19]. Edge dislocations have more effect on the thermal conductivity than screw dislocations [3].

## ACKNOWLEDGEMENTS

This research is supported by the U.S. Department of Energy, Office of High Energy Physics, through Grant No. DE-FG02-09ER41638.

## REFERENCES

- [1] W. Singer, A. Brinkmann, A. Ermakov, J. Iversen, G. Kreps, A. Matheisen, D. Proch, D. Reschke, X. Singer, and M. Spiwek, "Large grain superconducting RF cavities at DESY", In *AIP Conference Proceedings*, vol. 927, pp. 123–132, 2007.
- [2] T.R. Bieler, D. Kang, D.C. Baars, S. Chandrasekaran, A. Mapar, G. Ciovati, N.T. Wright, F. Pourboghrat, J.E. Murphy, and C.C. Compton, "Deformation mechanisms, defects, heat treatment, and thermal conductivity in large grain niobium", In *AIP Conference Proceedings*, vol. 1687, p. 020002(1–18). AIP Publishing, 2015.
- [3] W. Wasserbäch, "Low-temperature thermal conductivity of plastically deformed niobium single crystals", *Philosophical Magazine A*, vol. 38, no. 4, pp. 401–431, 1978.
- [4] W. Wasserbäch, "Lattice thermal conductivity and phonon-dislocation interaction in niobium and tantalum single crystals plastically deformed at intermediate temperatures", *Philosophical Magazine A*, vol. 52, no. 2, pp. 225–241, 1985.
- [5] S.K. Chandrasekaran, "Role of metallurgy in the thermal conductivity of superconducting niobium", Ph.D. Dissertation, Michigan State University, 2013.
- [6] P. Xu, T.R. Bieler, C.C. Compton, and N.T. Wright, "Temperature Excursions in Nb Sheets With Imbedded Delamination Cracks", in *Proc. SRF'15*, Whistler, Canada, Sep. 2015, paper MOPB007, pp. 82–85.
- [7] W. Wasserbäch, "Low-temperature thermal conductivity of pure and impure niobium and tantalum single crystals", *Physica Status Solidi (b)*, vol. 84, no. 1, pp. 205–214, 1977.
- [8] Alan Herries Wilson, "The theory of metals", *American Journal of Physics*, vol. 22, no. 4, pp. 243–244, 1954.
- [9] J. Bardeen, L. N. Cooper, and J. R. Schrieffer, "Theory of superconductivity", *Physical Review Letters*, vol. 108, pp. 1175–1204, 1957.
- [10] J. Bardeen, G. Rickayzen, and L. Tewordt, "Theory of the thermal conductivity of superconductors", *Physical Review Letters*, vol. 113, pp. 982–994, 1959.
- [11] P. Xu, T.R. Bieler, and N.T. Wright, "Effect Of Dislocations On the Thermal Conductivity Of Superconducting Nb", in *Proc. SRF'17*, Lanzhou,

- China, Jul. 2017, pp. 886–890. doi:10.18429/JACoW-SRF2017-THPB061
- [12] F. Koechlin and B. Bonin, “Parametrization of the niobium thermal conductivity in the superconducting state”, *Superconductor Science and Technology*, vol. 9, pp. 453–460, 1996.
- [13] P.G. Klemens, “The scattering of low-frequency lattice waves by static imperfections”, *Proceedings of the Physical Society. Section A*, vol. 68, no. 12, pp. 1113–1128, 1955.
- [14] S. Mazumder and A. Majumdar, “Monte Carlo study of phonon transport in solid thin films including dispersion and polarization”, *Journal of Heat Transfer*, vol. 123, no. 4, pp. 749–759, 2001.
- [15] R.B. Peterson, “Direct simulation of phonon-mediated heat transfer in a Debye crystal”, *Journal of Heat Transfer*, vol. 116, no. 4, pp. 815–822, 1994.
- [16] D. Lacroix, K. Joulain, and D. Lemonnier, “Monte Carlo transient phonon transport in silicon and germanium at nanoscales”, *Physical Review B*, vol. 72, no. 6, p. 064305(1–11), 2005.
- [17] J.P. Péraud and N.G. Hadjiconstantinou, “Efficient simulation of multidimensional phonon transport using energy-based variance-reduced Monte Carlo formulations”, *Physical Review B*, vol. 84, no. 20, p. 205331(1–15), 2011.
- [18] Peng Xu, Thomas R. Bieler, Neil T. Wright, “Modeling of lattice thermal conductivity of superconducting deformed niobium using monte carlo simulation”, in preparation, 2019.
- [19] W. Wasserbäch, “Electron–phonon scattering and low-temperature thermal conductivity of niobium and tantalum single crystals”, *Physica Status Solidi (b)*, vol. 127, no. 2, pp. 481–492, 1985.